Influence of pipe jacking excavation in overlying quicksand layer on surface settlement and numerical analysis

Peng Qi¹, Yi Huang^{1, 2, *}, Lijuan Cheng^{1, 2}, Yang Shen¹, Ru Yan^{1, 2}

¹Chengdu Engineering Corporation Limited, Chengdu, China

²Sichuan Urban Underground Space Survey Design and Construction Technology Engineering Laboratory, Chengdu, China

*Corresponding Author Email: p2020233@chidi.com.cn

Abstract. The cause of guicksand in soil depends on the nature of soil. Under the action of permeability, quicksand is easy to occur when the pore ratio of soil is large, the water content is large, the clay content is small, the silt content is large, the permeability coefficient is small and the drainage performance is poor. Therefore, quicksand phenomenon is easy to occur in fine sand, silt and loam, but whether quicksand phenomenon occurs or not also depends on certain external conditions, that is, the hydrodynamic pressure (permeability) generated by the seepage of groundwater in the soil. When the upward seepage force of unit granular soil is greater than or equal to its own gravity, the soil will suspend and move. In the process of underground engineering construction, if the problem of quicksand is not solved, the structure will displace with the flow of sand layer, which will change the bearing layer of the foundation and do great harm to the structure. This phenomenon should be eliminated. Practice shows that many accidents of underground structures are related to quicksand caused by the change of seepage conditions during construction. The disturbance of soil in pipe jacking construction is the fundamental cause of soil deformation. It destroys the original natural equilibrium state of soil, changes the stress-strain state of soil, and makes the undisturbed soil experience complex stress paths such as extrusion, shear and deformation. In this paper, a numerical model is established to analyze the surface settlement trend of pipe jacking in quicksand covered stratum, and the methods of grouting behind pipe jacking wall and excavation surface stability measures are verified to control the settlement measures in the construction process.

Keywords: Quicksand formation; Pipe jacking excavation; Grouting reinforcement; Surface subsidence.

1. Introduction

This part is about the sewage interception project. The sewage interception trunk pipe is divided into two sections, both of which are located in the west of Liangtan river. The first section starts from Longhua Road in the South and the inverted siphon outlet well in the north. The pipeline is about 815m long and d1800 in diameter[1]. The total length of the pipeline is about 2751.0m, and most of the pipe networks are deeply buried. According to the design drawing, the two sections (w32-w38) are constructed by pipe jacking method, with a buried depth of about 8.3-16.9m. The pipe jacking diameter is 1500, and the pipe jacking segment adopts C60 concrete.

The surface overburden along both banks of the river is mainly backfill and silty clay, and the underlying bedrock is sandstone, mudstone and siltstone of upper Shaximiao formation of middle jurassic system. The pipe jacking is simulated by concrete[2-3]. The stratum parameters selected in the model refer to the soil parameters given in the engineering geological exploration report, and physical soil parameters of all materials are shown in Table 1 below.

Table 1. Physical and mechanical parameters of each layer of soil.

Numble	soil layer	Unit weight (kN/m3)	Modulus of elasticity(kN/m2)	C(kPa)	ф(°)
1	back fill	18.98	6680	6.3	8.8
2	Sand layer	20.3	7560	2	5
3	Silty clay	18.9	9500	10.1	15
4	mudstone	21.8	55452	80	42

It is assumed that the construction pipeline is linear elastic material and the connection between pipelines is rigid [4-5]. According to the actual measurement of the project, the ground deformation is small. From the analysis of the current technical level of pipe jacking construction and the characteristics of construction area, the ground deformation caused by pipe jacking construction belongs to small deformation. Since the pipe jacking construction has little disturbance to the soil, and the stress and strain are small, the ultimate failure deformation of the soil generally does not occur, which is assumed to be elastic-plastic continuous deformation [6-7].

Because the friction resistance in the horizontal direction acts on the soil constantly [8], and the stress level after grouting is low, it is ignored in the calculation. Keep the front propulsive force of the working face as the fixed value, and the front propulsive force is simplified as the uniformly distributed load acting on the circular section [9-10]. In order to simplify the complexity of the three-dimensional finite element model, it is assumed that the element is vacant after jacking in one pipe joint length each time, and the jacking is regarded as a discontinuous and jumping process [11]. The three-dimensional model is shown in Fig.1 below:

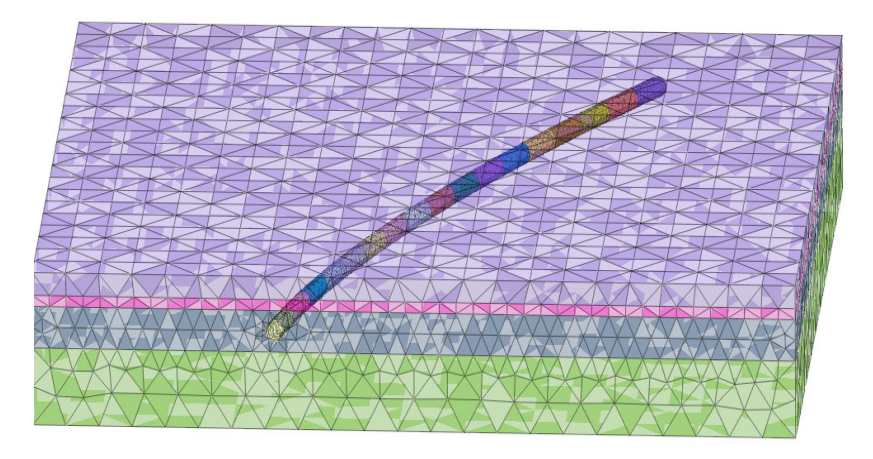


Figure 1. Relative space model between initiation position and tunnel.

2. Study on deformation model of flowing sand layer over pipe jacking

The overlying soil layer in the stratum where the pipe jacking tunnel is located is equivalent to the lower sandy soil by the layer method, and the thickness of the upper material in the double-layer foundation is replaced by a relevant equivalent thickness, the layer which can equivalent the composite stratum with uneven parameters to the homogeneous stratum with the same mechanical parameters, so as to simplify the problem. The thickness of the upper and lower strata is h, and the elastic modulus, poisson's ratio and internal friction angle are E, v, Φ respectively. The lower stratum can be equivalent to the current stratum soil with the same mechanical parameters as the upper stratum, and the equivalent thickness is expressed by the thickness h1 of the current stratum:

$$h_2 = h_2 (\frac{E2}{E1})^a \tag{1}$$

a is the index of the current layer, according to the actual measurement and empirical analysis of pipe jacking tunnel in similar stratum, a= 0.28 is taken. In this project, when the depth z is greater than h1, take the following formula [12]:

$$z' = h_1 + (z - h_1) \left(\frac{E_2}{E_1}\right)^a \tag{2}$$

For the most representative classical theory of stratum settlement caused by tunnel excavation, peck made regular statistics on a large number of tunnel excavation examples in 1969, put forward that the trend of land settlement deformation is normally distributed [13], and considered that the movement of soil medium leads to soil loss. According to the assumption that the soil is undrained and the volume is incompressible, the volume of normal distribution tank is equal to the volume of

soil loss, as shown in Figure 4, and the estimation formula of transverse land settlement is obtained [14].

$$S_x = S_{\text{max}} \exp(-\frac{x^2}{2i^2})$$
 (3)

$$S_{x} = S_{\text{max}} \exp(-\frac{x^{2}}{2i^{2}})$$

$$S_{\text{max}} = \frac{A_{x}}{i\sqrt{2\pi}} = \frac{\eta(\pi/4)D^{2}}{i\sqrt{2\pi}} = \frac{\eta\sqrt{\pi}D^{2}}{4\sqrt{2}i}$$
(4)

In there x is the distance from a point on the cross section to the tunnel axis; SX is the surface settlement value of the point; Smax is the maximum settlement of surface transverse settlement tank, as the volume of settlement tank per unit length. η is the formation loss rate. D is the tunnel excavation diameter, i is the horizontal distance from the ground point corresponding to the center line of the tunnel to the inflection point of the settlement curve, that is the half width of the settlement tank.

Based on the analysis of the measured data of surface settlement of similar pipe jacking construction in liquefiable sandy soil layer in the past, i is directly related to the buried depth of the bottom of the sand layer, and the width of the settlement groove increases with it. The width of the settlement trough has a nonlinear correlation with the increase of the excavation diameter of the tunnel jacking pipe, and a settlement trough width coefficient m is introduced [15].

$$i = m(z_n - z')D^n$$

$$S_{\text{max}} = \frac{\sqrt{\pi \eta}D^2}{4\sqrt{2}m(z_n - z')D^n} = \frac{\sqrt{\pi \eta}}{4\sqrt{2}m(z_n - z')}D^{2-n}$$

$$S_{x} = \frac{\sqrt{\pi \eta}}{4\sqrt{2}m(z_n - z')}D^{2-n} \exp(-\frac{x^2}{2m^2(z_n - z')^2D^{2n}})$$
(6)

The width coefficient of settlement tank is related to the thickness of sand layer and the equivalent buried depth of pipe jacking after conversion. By fitting the measured data of several actual pipe jacking projects in the same area and stratum with the least square method, the minimum value of the objective function is obtained by the least square method to find the function F(Zn, Z'). Through data fitting and trial calculation, so a constant coefficient M0 related to m is introduced here. The prediction formula of settlement curve is as follows:

$$S_{\text{max}} = \frac{\sqrt{\pi \eta}}{4\sqrt{2}m_0(\sqrt{z_n - 0.7z'})^{\frac{1}{3}}(z_n - z')} D^{2-n} \exp(-\frac{x^2}{2m_0^2(\sqrt{z_n - 0.7z'})^{\frac{2}{3}}(z_n - z')^2 D^{2n}})$$
(7)

In this project, according to the survey data, Zn is taken as 25m, and the overlying soil layer h1 is taken as 5m. According to the characteristics of sandy soil layer, n it is closely related to the construction method and settlement control measures, taking 0.5%. The value of m0 is obtained by numerical analysis and back calculation of settlement observation value. The rationality of the prediction model is verified.

3. Analysis and fitting of deformation results of quicksand layer overlying Pipe Jacking under different influencing factors

The existing theory shows that the maximum value of surface settlement in the process of excavation appears directly above the pipeline and gradually decreases outward along both sides. It is a curved surface of settlement trough on the surface, and most of the shape of settlement trough basically follows the assumption of positive distribution. Here, in order to verify the correctness of the model, for the calculation results obtained in the numerical simulation, select the unit data of a cross section of the pipeline to obtain the horizontal ground settlement curve of the section, and figs. 2-5 compare the settlement curves of the same section in different excavation stages during the excavation process.

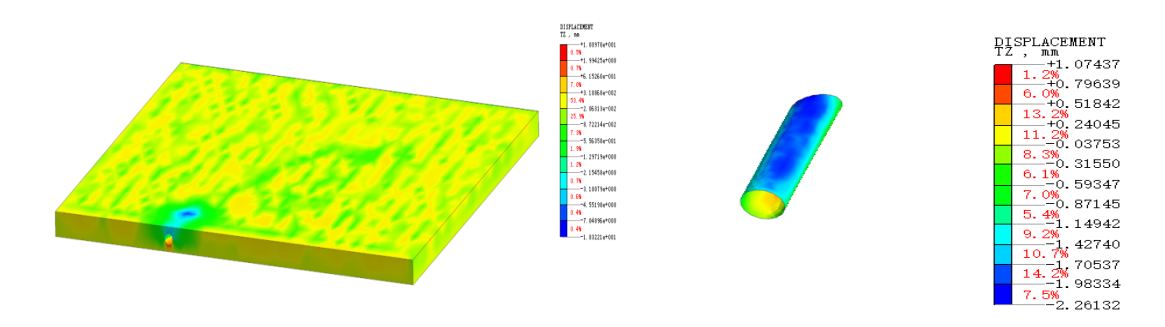


Figure 2. Vertical deformation in construction phase I (Dz= - 18.332mm)

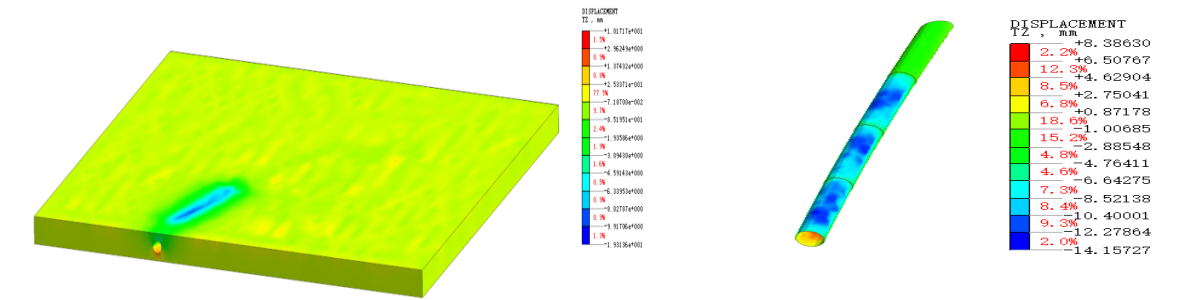


Figure 3. Vertical deformation in construction phase II (Dz= - 19.362mm)

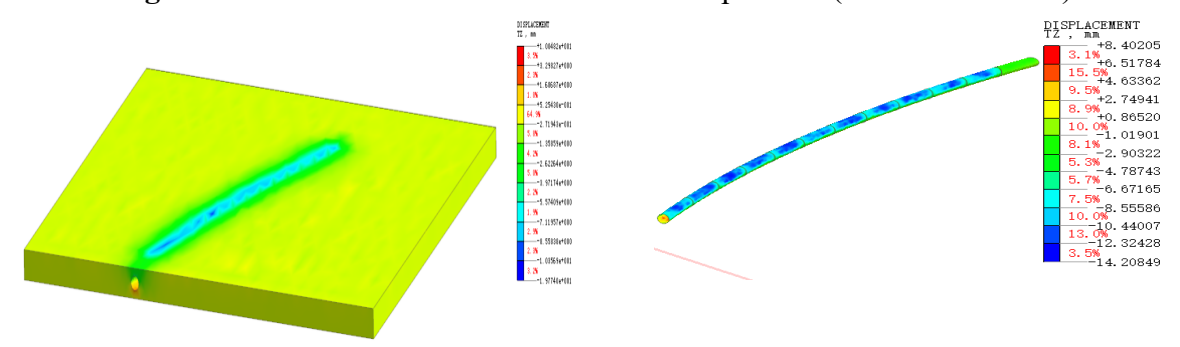


Figure 4. Vertical deformation in construction phase III (Dz= - 19.762mm)

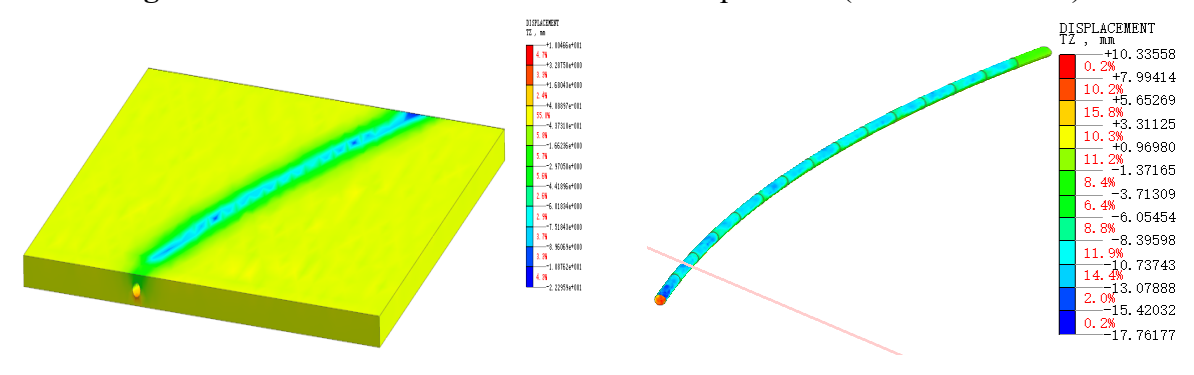
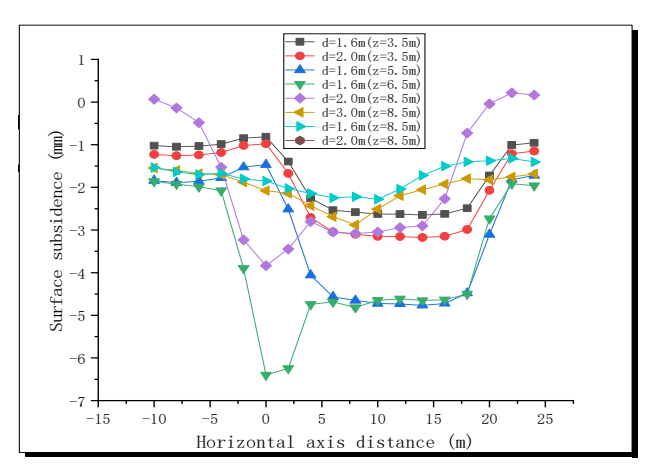


Figure 5. Vertical deformation in construction phase IV(Dz= - 22.962mm)

From figs.2-5 it can be seen that the excavation of pipe jacking has a relatively large and wide impact on the soil layer around the pipe, of which the greatest impact is at the vault of the excavation position of pipe jacking, and then gradually expand the influence range until it extends to the surface. Select representative nodes from the figure, intercept their data in the numerical model, the measuring points are located at the intersection of the 5th and 6th pipe joints. In addition, select measuring points with the same depth as the vault and the horizontal distance from the axis is 1 and 2 times the pipe diameter respectively for comparison shown in figs.6-7 below.



Buried depth z=3.0n
Buried depth z=5.0n
Buried depth z=10.0n

Figure 6. Variation curve of surface settlement under different working conditions

Figure 7. The trend of settlement trough in the modified prediction model

Through prediction and calculation, it is found that after the 2.0m diameter pipe jacking is completed, the settlement value and settlement range of the shallow buried pipe jacking are larger than that of the deep buried pipe jacking. Under the 3.0m shallow buried working condition, the maximum settlement reaches 28mm, and the settlement influence range is about 30m on both sides of the pipeline centerline. With the increase of the buried depth, the settlement has been controlled to a certain extent, and the settlement influence range has been greatly reduced. Under the actual working condition z = 9.5m, the maximum settlement is 18mm, which is about 36% lower than that under the condition of 3.0m buried depth. The influence range of settlement is about 12.0m on both sides of the pipeline centerline, which is about 60% lower than that under the condition of 3.0m buried depth. Under the condition of 19.0m buried depth, the influence range of settlement is not much smaller than that under the condition of 9.5m buried depth, but the total settlement is reduced by more than 50%. The prediction law of settlement is consistent with the prediction result of 1.6m diameter.

4. Conclusions

Through comparative calculation and extraction of the maximum particle vibration velocity, the monitoring results show that:

1) The section where the maximum particle vibration velocity peak is located is on the corresponding section near the blast hole (the free face). The calculation result is 10.74cm/s, such as the maximum vibration velocity in Y direction when t = 0.040s. On the same section, the velocity peak on the blasting face is greater than that on the back blasting face, such as the peak velocity of node 132 is 4.845cm/s.

2)The peak displacement on the blasting face of slope excavation, such as node 5662, is 34.43cm, and the maximum peak vibration velocity of the measuring point on the secondary lining reaches 10.74cm/s on the section. The influence on the completed structure of the left and right lines, the initial support and temporary support of the excavated tunnel chamber and the slope excavation from the tunnel and mine is analyzed and compared. With the passage of blasting time, the influence of displacement and acceleration decreases gradually, Therefore, it is very important to analyze the peak acceleration and maximum relative displacement as the on-site evaluation index and select whether the speed of each measuring point meets the blasting safety regulations.

3)The results show that there is no obvious correlation between the center distance of explosion and the charge quantity, and the maximum single shot charge quantity is strictly controlled. The particle vibration velocity of blasting vibration is related to the distance between blasting centers. With the increase of blasting center distance, the particle vibration velocity decreases gradually. Among the three-dimensional velocities of particle vibration, the horizontal radial velocity is the largest, and peak vibration velocity of the monitoring points is within the safe allowable range. The

monitoring results and attenuation law of blasting vibration have a certain reference value for the blasting mining of open-pit mines with similar terrain and geology.

References

- [1] Zhang Baisheng, Yang Zhiping, Yang Xuming, Zhang Shuai, Lin Jia. Presplit Blasting Technique in Treating Hard Overlying Strata: From Numerical Simulation to Field Practice[J]. Advances in Civil Engineering, 2021.
- [2] Zhang Hao, Li Tingchun, Wu Shuai et al. A study of innovative cut blasting for rock roadway excavation based on numerical simulation and field tests[J]Tunnelling and Underground Space Technology incorporating Trenchless Technology Research, 2022, 119.
- [3] Hao Jianchi, Ren Lifeng, Wen Hu et al. Experimental Study of Gangue Layer Weakening with Deep-Hole Presplitting Blasting[J] Shock and Vibration, 2021, 2021.
- [4] H.G. Naidu, R.K. Singhal Experience with cast blasting in Canadian surface coal mines[J] International Journal of Mining, Reclamation and Environment, 1989, 3(1).
- [5] Yong Wu, Wu Yong, Dai Yichang, Wang Shuaishuai, Wu Bo, Xu Shixiang, Wei Han. Analysis of Mutual Influence on Blasting Construction of Urban Shallow-buried Small Spacing Tunnels[J]. IOP Conference Series: Earth and Environmental Science, 2020, 525(1):
- [6] Wen-long Li; Xuan-ke Li; Ke Shen; Hui-tao Xu; Jian-guang Guo; Yong Wu Preparation and characterization of graphitized polyimide film/epoxy resin composites with high thermal conductivities [J] Carbon, 2022.
- [7] Yong Wu; Wei Li; Xiaoming Fan; Binjun Wang Entity-Context and Relation-Context Combined Knowledge Graph Embeddings [J] Arabian Journal for Science and Engineering, 2021.
- [8] Yong Wu; Xinpo Li; Lei Zhu Fracture mechanism of rock collapse in the freeze-thaw zone of the eastern Sichuan-Tibet Mountains under seasonal fluctuating combinations of water and heat [J] Natural Hazards, 2021
- [9] Yuncan Chen; Xin Huang; Yingying Xu; Jianglian Li; Ruizhi Lai; Mei Guan; Yong Wu Ru (II)-Catalyzed C–H Activation Reaction between 2-Phenyl-quinazolinone and Vinylene Carbonate [J] SYNLETT, 2021.
- [10] Xiaoming Guan, Xuchun Wang, Zhen Zhu, Liang Zhang, Hongxian Fu. Ground Vibration Test and Dynamic Response of Horseshoe-shaped Pipeline During Tunnel Blasting Excavation in Pebbly Sandy Soil[J]. Geotechnical and Geological Engineering, 2020(prepublish).
- [11] Seong-Seung Kang, Hyongdoo Jang. A case study on tunnel blasting design evaluation considering blast damage zone[J]. Science and Technology of Energetic Materials, 2020, 81(No.4).
- [12] Zihan Liu, Nan Jiang, Jinshan Sun, Yuqing Xia, Guopeng Lyu. Influence of tunnel blasting construction on adjacent highway tunnel: A case study in Wuhan, China[J]. International Journal of Protective Structures, 2020, 11(3).
- [13] Xiaoming Guan, Liang Zhang, Yuwen Wang, Hongxian Fu, Jianyong An. Velocity and stress response and damage mechanism of three types pipelines subjected to highway tunnel blasting vibration[J]. Engineering Failure Analysis, 2020, 118.
- [14] Xiaoxu Tian, Zhanping Song, Junbao Wang. Study on the propagation law of tunnel blasting vibration in stratum and blasting vibration reduction technology[J]. Soil Dynamics and Earthquake Engineering, 2019, 126(C).
- [15] Nan Jiang, Tan Gao, Chuanbo Zhou, Xuedong Luo. Safety assessment of upper buried gas pipeline under blasting vibration of subway tunnel: a case study in Beijing subway line[J]. Journal of Vibroengineering, 2019, 21(4).